Qubit-Efficient Variational Quantum Algorithms for Image Segmentation

Supreeth Mysore Venkatesh[1,2], Antonio Macaluso[2], Marlon Nuske[3],
Matthias Klusch[2], Andreas Dengel[1,3]

[1]*University of Kaiserslautern-Landau (RPTU)*, Kaiserslautern, Germany
[2]*German Research Center for Artificial Intelligence (DFKI)*, Saarbruecken, Germany
[3]*German Research Center for Artificial Intelligence (DFKI)*, Kaiserslautern, Germany
supreeth.mysore@rptu.de, antonio.macaluso@dfki.de, marlon.nuske@dfki.de,
matthias.klusch@dfki.de, andreas.dengel@dfki.de

Abstract—Quantum computing is expected to transform a range of computational tasks beyond the reach of classical algorithms. In this work, we examine the application of variational quantum algorithms (VQAs) for unsupervised image segmentation to partition images into separate semantic regions. Specifically, we formulate the task as a graph cut optimization problem and employ two established qubit-efficient VQAs, which we refer to as Parametric Gate Encoding (PGE) and Ancilla Basis Encoding (ABE), to find the optimal segmentation mask. In addition, we propose Adaptive Cost Encoding (ACE), a new approach that leverages the same circuit architecture as ABE but adopts a problem-dependent cost function. We benchmark PGE, ABE and ACE on synthetically generated images, focusing on quality and trainability. ACE shows consistently faster convergence in training the parameterized quantum circuits in comparison to PGE and ABE. Furthermore, we provide a theoretical analysis of the scalability of these approaches against the Quantum Approximate Optimization Algorithm (QAOA), showing a significant cutback in the quantum resources, especially in the number of qubits that logarithmically depends on the number of pixels. The results validate the strengths of ACE, while concurrently highlighting its inherent limitations and challenges. This paves way for further research in quantum-enhanced computer vision.

Index Terms—Quantum algorithms, variational circuits, image segmentation, combinatorial optimization

I. INTRODUCTION

Variational Quantum Algorithms (VQAs) aim to leverage NISQ devices for practical uses through a hybrid quantum-classical approach [1]. VQAs address classical problems, which lack polynomial-time solutions but have verifiable answers, showcasing their potential for real-world applications. One application area that highlights the potential of VQAs is in solving Quadratic Unconstrained Binary Optimization (QUBO) problems, an NP-Hard class of optimization problems with applications in various domains, including logistics, finance, and machine learning [2]. The Quantum Approximate Optimization Algorithm (QAOA) represents a notable example of VQAs applied to such challenges [3]. While classical computers can handle QUBO for instances with several thousand variables, running QAOA on similar tasks requires thousands of qubits, a requirement that appears out of reach given the constraints of near-term quantum technology. The scalability of QAOA is inherently limited by the linear relationship between the number of binary variables in QUBO problems and the number of logical qubits required, underscoring the pressing need to explore more efficient encoding strategies. These strategies are designed to mitigate the hardware limitations of current quantum devices while simultaneously unlocking new possibilities for efficiently addressing complex tasks that classical computing capabilities cannot solve.

In this work, we adapt two existing variational quantum algorithms, which we refer to as *Parametric Gate Encoding (PGE)* [4] and *Ancilla Basis Encoding (ABE)* [5], to address the task of image segmentation formulated as a combinatorial optimization problem [6]. *PGE* encodes the segmentation solution in the parameterized gates exerted in the quantum ansatz, while *ABE* [5] uses the probability distribution of the qubits' basis states for encoding the solution [4]. Furthermore, we propose an enhancement of *ABE*, termed *Ancilla Cost Encoding (ACE)* that uses a problem-specific cost function and demonstrates an improved performance. Importantly, these
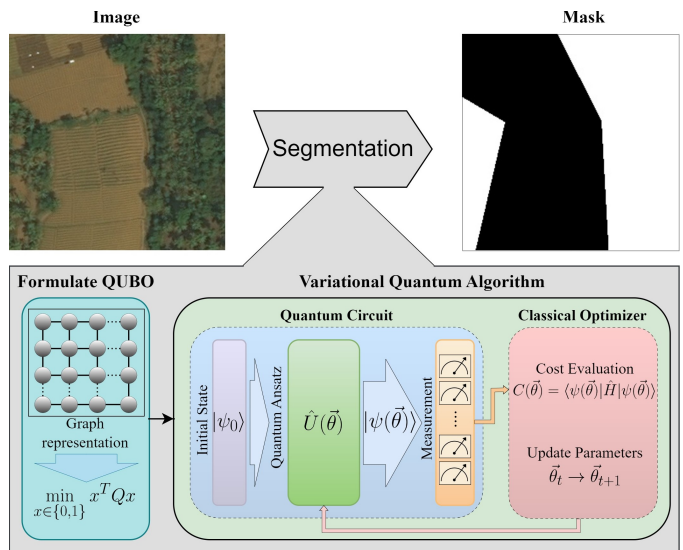

Fig. 1.The figure depicts an architecture for segmenting an image. Generating a graph representation of the image, the distinct semantic regions in the image are identified by finding the minimum cut in the graph that can be formulated as Quadratic Unconstrained Binary Optimization (QUBO). The QUBO problem is subsequently solved using a VQA by optimizing the circuit parameters that incidentally explore an exponentially large solution space to locate the global optimum, which can be decoded as the segmentation mask.

algorithms require exponentially fewer qubits than QAOA and its variants, scaling logarithmically with the number of image pixels. This represents a significant improvement in scalability for image segmentation tasks using VQAs. We begin by reformulating the image segmentation problem as a graph partition problem, subsequently framed as a QUBO. The experiments are focused on analyzing the solution quality and the efficiency of various classical optimizers for these algorithms. We also provide a theoretical analysis of essential quantum resource requirements as a function of the number of pixels of the input image. For a well-rounded study, we also discuss the specific limitations of each approach. Our findings open new research directions for leveraging quantum computing in computer vision, particularly in the optimization of quantum resources for complex computational tasks.

II. RELATED WORKS

Supervised deep learning models have set benchmarks in image segmentation by leveraging precisely annotated data. However, the collection of such labeled datasets faces hurdles, including significant annotation time and costs, the necessity of specialized knowledge, and issues scaling to vast datasets, not to mention the inconsistencies arising from variable interpretations by different annotators [7]. These limitations highlight the importance of unsupervised segmentation methods, especially valuable for leveraging extensive unlabeled data pools [8]. Nonetheless, the computational demand of some unsupervised techniques, like graph-based segmentation [9], presents a significant limitation, making these tasks ideal targets for quantum computing to promise more efficient solutions.

A wide range of research has explored the use of quantum algorithms for computer vision tasks, primarily focusing on image classification [10]–[13] and matching [14], [15]. Additionally, quantum-inspired classical techniques have been applied to segmentation [16] and edge-detection [17], [18], blending quantum concepts with traditional computing infrastructure. In particular, quantum annealers and hybrid quantum-classical approaches have demonstrated promise for image segmentation, converting these challenges into a QUBO problem [6], [19], [20]. Despite their innovative methods, they face limitations in scalability and are constrained by the current capabilities of quantum annealers for handling high-resolution images.

In contrast, our work focuses on leveraging the versatility of VQAs, particularly suited for NISQ devices, to overcome the scalability limitations in existing quantum and hybrid approaches. Unlike methods requiring extensive quantum resources or fault tolerance, we adapt established encoding strategies to harness the potential of quantum circuits in enhancing computer vision techniques, specifically image segmentation, through efficient quantum resource utilization.

III. PRELIMINARIES

The segmentation process involves representing an input image as a lattice graph with nodes corresponding to pixels and edges representing pixel similarity. The approach is particularly interesting as it can capture both spatial and spectral information in the image [9]. Segmentation seeks to partition this graph's vertices into mutually exclusive subsets, such that the total weight of the edges connecting vertices from one subset to another is minimized, defined as:

$$\text{MINIMUMCUT}(G) = \arg\min_{A,\overline{A}} \sum_{i \in A, j \in \overline{A}} w(v_i, v_j) \quad (1)$$

where G denotes the graph and $w(v_i, v_j)$ is the weight of the edge connecting the nodes v_i and v_j. Given the NP-hard nature of the min-cut problem for arbitrary weights, classical solutions become computationally challenging, motivating the reformulation into a QUBO problem to exploit the power of quantum computers [21].

Example: Let's consider an image of size 2×2, which is converted to a grid graph with a one-to-one mapping of the pixels to the vertices. The edge weights are assigned as the similarity measure between the neighboring pixels. Finding the minimum cut in this grid graph will eventually give the segmentation of the image.
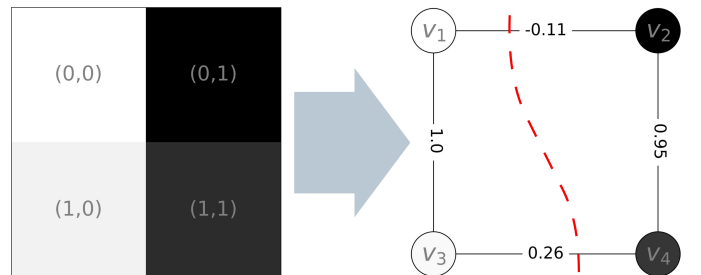

Fig. 2. Transformation of a 2×2 pixel image into a grid graph, where edge weights indicate pixel similarity. The red dashed line depicts the edges that are cut to partition the graph.

Focusing on the capabilities of existing NISQ technology, we target near-optimal solutions as they are often tolerable for downstream computer vision tasks. With n vertices, the binary encoding of each vertex in graph G facilitates the representation of potential solutions as vector $\in \{0,1\}^n$ delineating the vertices into two disjoint subsets, with edges intersecting these subsets identified as cuts. Such an encoding allows to reformulate the minimum cut as a QUBO without loss of generality as [22], [23]:

$$\vec{x}^* = \arg\min_{\vec{x}} \sum_{1 \leq i < j \leq n} x_{v_i}(1 - x_{v_j})w(v_i, v_j)$$
$$= \arg\min_{\vec{x}} \ \vec{x}^T Q \vec{x} \quad (2)$$

where $\vec{x}^*$ represents the optimal solution for the minimum cut of G. The construction of the $Q \in \mathcal{R}^{n \times n}$ matrix is derived from the coefficients of terms in the quadratic expression of the binary variables x_{v_i} for $i \in \{1, 2, ..., n\}$ obtained by substituting the edge weights $w(v_i, v_j)$ and simplifying.

QAOA, a special case of the Variational Quantum Eigensolver (VQE) [24], is designed for QUBO problems, implementing a parameterized quantum circuit to approximate the problem's ground state. The binary encoding strategy employed for solving the image segmentation problem using QAOA leads to scalability challenges of representing high-resolution images with individual qubits for each pixel. In

contrast to the problem-specific ansatz of QAOA, the methods we explore use a problem-agnostic ansatz. This gives rise to a need for efficient encoding strategies within the VQA framework to address image segmentation, requiring fewer qubits and offering scalable solutions for practical applications.

IV. METHODS

In this section, we will explain the two methods and describe a new approach to obtain the segmentation of an image employing innovative encoding strategies for solving the QUBO problem.

A. Parametric Gate Encoding (PGE)

Given a grid graph G constructed from the input image, the Laplacian matrix L_G provides a compact representation of the graph's structure, capturing information about the connectivity and degree of each vertex, and is given by $L_G = D_G - A_G$, where D_G is the degree matrix, a diagonal matrix with vertex degrees $d(v_i)$ for v_i on the diagonal, and A_G is the adjacency matrix, a square matrix where the element $A_G[i,j]$ is the weight of the edge between the vertices v_i and v_j. If the dimension of the matrix L_G is not a power of 2, without loss of generality, we pad the matrix with zeroes to the nearest power of 2 to ensure that the matrix dimensions are compatible with the quantum register, as quantum states are represented in a Hilbert space of dimension n for $\log_2(n)$ qubits. Since the Laplacian is a symmetric matrix consisting of real-valued edge weights for undirected weighted graphs, it is also Hermitian and thus serves as a suitable quantum observable [4].

The *PGE* method constructs a parameterized quantum circuit with $n' = \lceil \log_2(n) \rceil$ qubits, initializing with Hadamard gates for equal superposition and applying a diagonal gate as the ansatz which can be expressed as [4]:

$$\hat{U}(\vec{\Theta}) = \begin{pmatrix} \exp(i\pi f(\theta_1)) & 0 & \cdots & 0 \\ 0 & \exp(i\pi f(\theta_2)) & \cdots & 0 \\ \vdots & \vdots & \ddots & \vdots \\ 0 & 0 & \cdots & \exp(i\pi f(\theta_{2^{n'}})) \end{pmatrix}$$
(3)

where $\vec{\Theta} = (\theta_1, \theta_2, ...\theta_{2^{n'}})$, and $\theta_i \in [0, 2\pi]$ for $i \in \{1, 2, ..., 2^{n'}\}$ and f is piecewise function defined as:

$$f(\theta_i) = x_{v_i} = \begin{cases} 0 & 0 \leq \theta < \pi \\ 1 & \pi \leq \theta < 2\pi \end{cases} \forall i \in \{1, 2, ..., 2^{n'}\}$$
(4)

with $n' - 2$ two-qubit CNOT gates and n' single-qubit parametric gates, where each parametric gate in the variational ansatz encodes a binary decision for the segmentation mask. With L_G as the observable, the measurement operation is performed, and the energy of the system is evaluated as:

$$C(\vec{\Theta}) = \frac{2^{n'}}{2} \langle \psi(\vec{\Theta})|L_G|\psi(\vec{\Theta}) \rangle$$
(5)

Since L_G is also a Hermitian matrix, it is decomposed into a linear combination of tensor products of Pauli matrices, enabling the evaluation of the quantum observable corresponding to the graph structure. The parameters $\vec{\Theta}$ are adjusted iteratively using a classical optimizer to minimize the cost

function (Eq. 5). The optimal parameters $\vec{\Theta} = \{\theta_1, \theta_2, ...\theta_{2^{n'}}\}$ are decoded to binary values (Eq. 4), obtaining the minimum cut and eventually the binary segmentation mask of the image.

B. Ancilla Basis Encoding (ABE)

For an image with n pixels to be segmented, the QUBO problem formulated will also have n variables. The *ABE* [5] strategy uses only $\log_2(n) + 1$ number of qubits, where the $\log(n)$ qubits are called the register qubits and the additional qubit is termed as the ancilla qubit. Using a hardware efficient ansatz where each layers consists of $\log_2(n)$ CNOT gates between adjacent qubits and $\log_2(n) + 1$ parametric $R_y(\theta)$ gates for each qubit, the quantum state is represented as:

$$|\psi(\vec{\Theta})\rangle = \sum_{i=1}^{n} \beta_i(\vec{\Theta})(a_i(\vec{\Theta})|0\rangle_a + b_i(\vec{\Theta})|1\rangle_a) \otimes |\phi_i\rangle_r$$
(6)

where $|\phi_i\rangle_r$ are the computational basis states of the register qubits, $|0\rangle_a$ and $|1\rangle_a$ are the states of the ancilla qubit, a_i and b_i are the amplitudes for the ancilla qubit, and $\beta_i(\vec{\Theta})$ are coefficients dependent on variational parameters $\vec{\Theta}$. The expectation measurements obtain a probability distribution over the basis states of the qubits in the circuit and the solution is decoded as:

$$x_{v_i} = \begin{cases} 0 & |a_i|^2 > |b_i|^2 \\ 1 & otherwise \end{cases}$$
(7)

where $|a_i|^2 + |b_i|^2 = 1$.

The probability of finding the optimal solution increases as the number of measurements tends to ∞ [5]. While it may appear impractical, for relatively small quantum circuits, the number of measurement operations only needs to be large enough to adequately approximate the optimal probability distribution; it does not necessarily need to be ∞. Additionally, well-established VQAs like QAOA are guaranteed to find the optimal solution only as the depth of the corresponding quantum circuit tends to infinity. According to the ABE approach, the quantum circuit is typically initiated by a layer of Hadamard gates to generate a uniform superposition, followed by a hardware-efficient ansatz applied to evolve the quantum state. For the parameters $\vec{\Theta}$, the cost is given by:

$$C(\vec{\Theta}) = \sum_{i,j=1}^{n} Q_{ij} \frac{\langle \hat{P}_i^1 \rangle_{\vec{\Theta}} \langle \hat{P}_j^1 \rangle_{\vec{\Theta}}}{\langle \hat{P}_i \rangle_{\vec{\Theta}} \langle \hat{P}_j \rangle_{\vec{\Theta}}} (1 - \delta_{ij}) + \sum_{i=1}^{n} Q_{ii} \frac{\langle \hat{P}_i^1 \rangle_{\vec{\Theta}}}{\langle \hat{P}_i \rangle_{\vec{\Theta}}}$$
(8)

where $\hat{P}_i$ are projectors over the basis states of the register qubits $|\phi_i\rangle_r$, irrespective of the state of the ancilla qubit, $\delta_{ij} = 1$ when $i = j$ and Q is the matrix representing the QUBO problem. The objective is to find a binary vector $\vec{x}^*$ that minimizes $\vec{x}^\top Q \vec{x}$. The expectation values $\langle \hat{P}_i \rangle$ embody the probabilities of observing the qubit states that encode the binary variables x_{v_i} of the QUBO solution vector $\vec{x}$. The projectors P_i and $\hat{P}_i^1$ are operators that map the quantum state onto the respective basis states of the register qubits, with P_i aligning with the state that encodes $x_{v_i} = 1$. $\hat{P}_i^1$ modifies this to include the state of the ancilla qubit [5]. Finally, an optimizer running on a classical computer optimizes the variational parameters $\vec{\Theta}$ to minimize $C(\vec{\Theta})$ (Eq. 8).
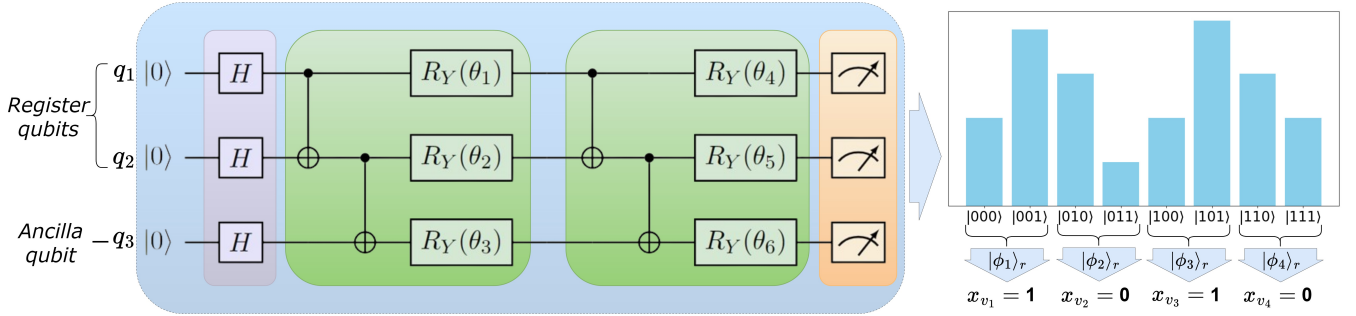
Fig. 3. Quantum circuit of *ABE/ACE* for finding the segmentation mask of the example image in Fig. 2. illustrating the encoding of the solution of a QUBO problem of size 4 into a quantum state facilitated by 3 qubits: q_1, q_2 are the register qubits and q_3 is the ancilla qubit. The circuit initialization employs Hadamard gates to induce superposition across all qubits, followed by two layers of hardware-efficient ansatz with entanglement and rotation gates parameterized by $\vec{\Theta}$. Executing and measuring the circuit obtains a probability distribution over the basis states. For the basis states whose register qubits are the same encodes the value of the binary variable. For example, with the register qubit basis states $|\phi_1\rangle_r = |00\rangle$, we obtain the value $x_{v_1} = 1$ as the probability of the ancilla qubit in state $|1\rangle > |0\rangle$ (Eq. 7).

C. Adaptive Cost Encoding (ACE)

We propose a modified cost function using the same encoding strategy as *ABE*. During each iteration of the optimization, once we measure the circuit multiple times, we get a probability distribution that can be decoded into a binary vector $\vec{x}$ that represents a possible solution. Instead of using the cost function in Eq. 8, we can make use of the min-cut problem's cost function i.e.,

$$C(\vec{x}) = \sum_{1 \leq i < j \leq n} x_{v_i}(1 - x_{v_j})w(v_i, v_j) \qquad (9)$$

where $\vec{x} = x_{v_1}, x_{v_2}, ..., x_{v_n}$ such that $x_{v_i} \in \{0,1\}$ given by Eq. 7, and $w(v_i, v_j) \; \forall \; i, j \in \{1, 2, ..., n\}$ is the edge weight between v_i and v_j. In case of *ABE*, given two sets of parameters, say $\vec{\Theta}_1$ and $\vec{\Theta}_2$, obtaining the binary vectors $\vec{x}_1$ and $\vec{x}_2$ respectively (Eq. 6 and 7), if $C(\vec{\Theta}_1) < C(\vec{\Theta}_2)$ (Eq. 8) does not always guarantee that $C(\vec{x_1}) < C(\vec{x_2})$ (Eq. 9) which implies that the optimal circuit parameters may not correspond to the minimum cut. Whereas, *ACE* guarantees that the optimization process obtains the solution of the original problem, i.e., the optimal circuit parameters $\vec{\Theta}$ implies the corresponding $\vec{x}$ minimizes the minimum cut cost function (Eq. 9). Moreover, the QUBO formulation of the original problem also becomes obsolete as the cost function directly involves the weights of the edges in the graph and not the QUBO coefficients. In the following section, through our experiments, we demonstrate ACE to have improved trainability, a strong tendency to find better solutions and a more consistent behavior using different optimizers with our proposed problem-specific cost function compared to *ABE*.

Furthermore, the adaptive cost function can be extended to other combinatorial optimization problems where the problem formulation expresses the solution as a binary vector and uses the original cost function. This approach can be crucial for tasks where the optimization problem includes constraints and reformulating the problem as a QUBO involves integrating the constraints as penalty terms into the cost function with an appropriate penalty coefficient, eventually not depicting the original problem [25]. Even an optimal penalty coefficient should be set, while a very low value can lead to the consideration of an invalid binary vector as a solution, or

a high value can cause any valid solution to be considered optimal. Whereas, *ACE* allows finding the optimal solution of the original problem without modifying the cost function or the constraints, by setting a high or low cost for binary vectors that do not obey the constraints depending on whether the problem is minimization or maximization respectively.

Example: Considering again the 2×2 image from the previously discussed example (Fig. 2).

For *PGE*, the Laplacian L_G is of size 4×4 and the encoding scheme uses a quantum circuit with just 2 qubits. The circuit consists of an initial layer of Hadamard gates, followed by the ansatz $\hat{U}(\vec{\Theta})$ (Eq. 3) which is a diagonal gate of size 4×4. With L_G as the observable, optimizing the cost function and obtaining the optimal circuit parameters $\theta_1^*, \theta_2^*, \theta_3^*, \theta_4^*$, we can decode the binary mask $x_{v_1}^*, x_{v_2}^*, x_{v_3}^*, x_{v_4}^*$ (Eq. 4). While this approach is efficient in terms of the number of qubits, the main drawback is the number of parameters which implies an overhead in the classical optimization process.

Figure 3 represents the quantum circuit and the encoding strategy for solving this example. In the cost function (Eq. 8) of *ABE*, the term $\langle \hat{P}_i \rangle_{\vec{\Theta}}$ is the probability of the basis state $(|0\rangle_a + |1\rangle_a) \otimes |\phi_i\rangle_r$, and the term $\langle \hat{P}_i^1 \rangle_{\vec{\Theta}}$ is the probability of the state $|1\rangle_a \otimes |\phi_i\rangle_r$, where $|0\rangle_a$ and $|1\rangle_a$ are the basis states of the ancilla qubit. Updating the parameters, a unitary evolution is performed over the state $|\psi_0\rangle$ which produces a new state $|\psi_1(\vec{\Theta})\rangle = \hat{U}_1(\vec{\Theta})|\psi_0\rangle$. The optimization iteratively adjusts $\vec{\Theta}$, and each iteration involves running the quantum circuit and evaluating the cost function. A classical optimizer is used to find the optimal parameters $\vec{\Theta}_{\text{opt}}$ that minimize the cost function $C(\vec{\Theta})$. Decoding the final quantum state $|\psi_1(\vec{\Theta}_{\text{opt}})\rangle$, we obtain a binary vector $\vec{x}$ which represents the solution of the QUBO problem, which is the binary segmentation mask of the given image. Whereas in the case of *ACE*, at each iteration of the optimizer, the measurement is decoded to get the binary vector $\vec{x}$, and the value of the cost function in Eq. 9 is minimized by optimizing the circuit parameters $\vec{\Theta}$.
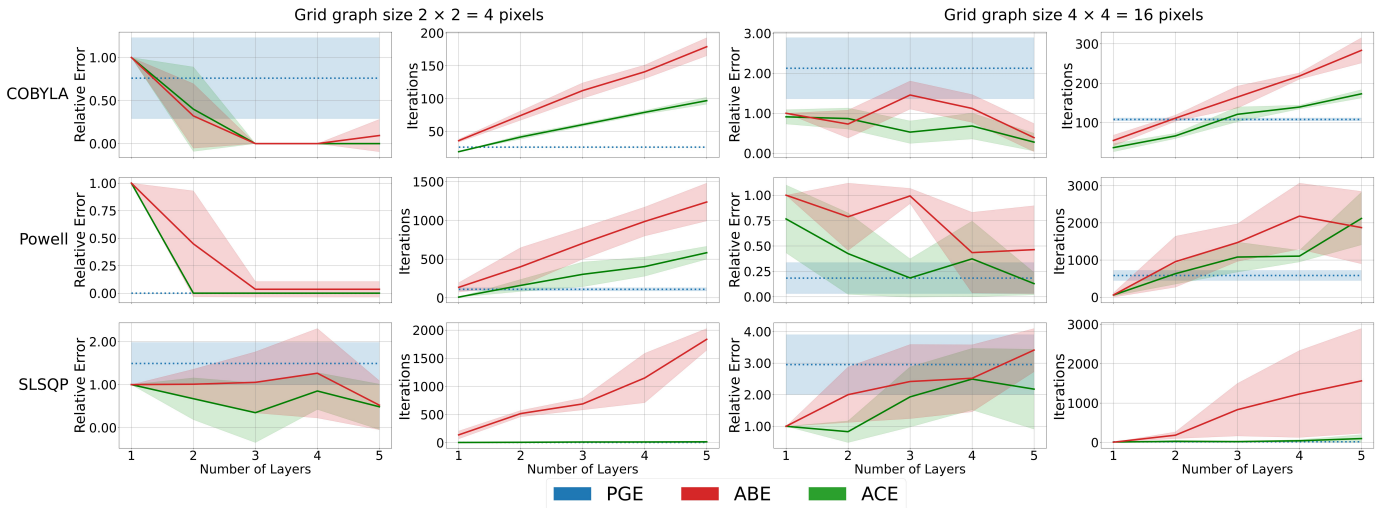
Fig. 4. The figure illustrates the performance of *PGE*, *ABE* and *ACE* for finding the minimum cut on grid graphs of size 2×2 and 4×4 with the layers in the ansatz of the quantum circuit ranging from 1 to 5 in terms of the solution quality and the efficiency of the optimization process. The plots show the average and standard deviation of the relative errors in the obtained solution's cost as a measure of quality and the number of iterations to quantify the trainability using COBYLA, Powell, and SLSQP optimizers.

V. EXPERIMENTS

A. Experimental Settings

PGE, *ABE*, *ACE* algorithms are implemented in Qiskit framework, and the experiments are executed on a classical computer using Qasm simulator. Inspired from the existing literature [6], the synthetic dataset consist of square grid graphs by sampling edge weights from a uniform distribution in the range [-1,1], and the experiments were executed for sizes 2×2 i.e., 4 pixels, and 4×4 i.e., 16 pixels, as all the approaches discussed previously behave similarly for images of sizes from $\log_2(n+1)$ pixels up to size n. For the reproducibility of results and fair comparison, we have executed the experiments using 5 fixed seeds for generating the problem instances and the initial values for the parameters of the variations circuits. We evaluated the local optimizers from the Scipy library, detailing the results for COBYLA, Powell, and SLSQP. For *ABE* and *ACE*, we increased the number of layers up to a maximum of 5, allowing additional layers to introduce more parameters for optimization, causing significant overhead for the classical optimizer. To ensure the solution quality improves with an increased number of measurements [5], we conducted our experiments with $65,536$ measurements for each optimization iteration.

We benchmarked the solution quality and optimization efficiency of *PGE*, *ABE*, and *ACE* against the results from *Gurobi*, known for its effectiveness in solving combinatorial optimization problems. Solution quality was evaluated by calculating the relative error of the minimum cut value from the VQAs relative to *Gurobi*, defined as Relative Error $= \frac{|C_{\text{VQA}} - C_{\text{gurobi}}|}{|C_{\text{gurobi}}|}$. We measured optimization efficiency by the number of iterations needed for the cost function, which directly correlates with the frequency of quantum circuit executions. *PGE* uses a constant-depth quantum circuit and shows no variance across different layers of the ansatz. The software for these experiments was developed using *Python 3.10*.

B. Results

Figure 4 illustrates the experiments for synthetically generated problems fixing 5 seeds with layers $\in [1,5]$ using different classical optimizers. We see that using our modified cost function in *ACE* parameterized by the binary vector decoded from the measurement of the quantum circuit helps the optimizer decide upon the optimal solution much quicker than *ABE* that uses a cost function parameterized directly by the probability distribution obtained from the measurement process. Moreover, the training is more consistent for *ACE* as we observe minimal variations in the number of iterations and the quality across 5 seeds. The number of iterations is consistently lower for *ACE* as the different costs explored during the optimization are discrete as the minimum cut is a combinatorial optimization problem, lowering the possibilities to explore in contrast to *ABE* where the optimization landscape is not only non-convex but also infinitely many values are explored. However, certain optimizers, such as SLSQP, demonstrate limitations when faced with a higher number of layers, struggling with the increased overhead from optimizing a larger parameter set and thus proving unsuitable for scenarios demanding extensive parameter optimization. Although, *PGE* can be seen performing better with Powell optimizer, the number of parameters optimized is exponential to that of qubits. Therefore, we extend our experiments using a more robust classical optimizer to prove the efficacy of *ACE* in terms of the number of parameters to optimize.

Given the non-convex and non-differentiable nature of the problem, classical optimizers focused on local optimization may not always secure the global optimal solution. Although inefficient in terms of runtime, using a metaheuristic optimizer like *Differential Evolution* could be more effective as the cost function lacks smoothness. This approach helps illustrate that even a single layer of *ACE*, with just a logarithmic number of parameters equal to the number of qubits, can capably represent the solution to the original problem.

Seed	Size	Iterations	Execution Time (s)	Obtained Value	Exact Value
111	4	3463	236.13	-1.13	-1.13
	16	14601	1320.92	-1.54	-1.54
222	4	4966	362.44	-0.62	-0.62
	16	75225	3557.49	-3.97	-3.97
333	4	5439	379.46	-1.16	-1.16
	16	40287	3477.47	-3.57	-3.57
444	4	9174	622.83	-1.20	-1.20
	16	75201	3797.97	-2.19	-2.19
555	4	3737	268.69	-1.86	-1.86
	16	75201	4202.49	-2.56	-2.56

TABLE I. Table details performance metrics for *ACE* with a single layer, optimized using a differential evolution strategy. It includes reproducibility seeds, image sizes denoted by pixel count, total optimizer iterations, computational runtimes in seconds, and minimum cut values obtained by *ACE* alongside those calculated through an exhaustive search for validation.

The results in Table I reveal that *ACE* can solve a combinatorial optimization problem consisting of n variables by optimizing only $\log_2(n) + 1$ parameters. From a classical perspective, treating the quantum circuit as a black box, *ACE* allows to reformulate an NP-Hard problem of size n as a multivariate optimization problem of size $O(\log_2(n))$ leveraging the power of quantum computing. In contrast, *PGE* requires to optimize the same number of real-valued parameters and also uses more number of gates.

C. Theoretical Analysis

Here we perform an analysis on the scaling of *QAOA*, *PGE*, *ABE* and *ACE* based on the metrics typically considered for evaluating the scalability of VQAs. In particular, we provide the complexities of the discussed NISQ algorithms for image segmentation in terms of qubit complexity which is a major bottleneck for present-day applicability, the number of two-qubit *entanglement gates* is vital to understanding the error rates due to decoherence, the number of *parametric gates* is crucial for assessing the overhead on the classical optimizer, and the circuit *depth* which is the longest sequence of quantum gates applied from the input till the measurement operation which provides an estimate of circuit execution time.

Method	Qubit complexity	Entanglement gates	Parametric gates	Circuit depth
QAOA	$O(n)$	$O(n^2)$	$O(Ln)$	$O(Ln^2)$
PGE	$\log_2(n)$	$n-1$	n	n
ABE/ACE	$\log_2(n)+1$	$L(\log_2(n))$	$L(\log_2(n)+1)$	$L(\log_2(n)+1)$

TABLE II. Scalability analysis of VQAs for solving QUBO problems in terms of quantum resources.

Table II provides a theoretical scalability analysis, where n is the number of binary variables in QUBO and L is the number of layers in the ansatz of the quantum circuit. Acknowledging the qubit limitations in emerging quantum technologies, the scalability of the methods introduced here, excluding QAOA, is notably superior. They potentially allow for the segmentation of a $1-$megapixel image, equivalent to 2^{20} pixels, utilizing merely 20 qubits.

VI. DISCUSSION AND CONCLUSION

The segmentation methods explored in this paper demonstrate substantial scalability in terms of quantum resources compared to well-known variational quantum algorithms like QAOA. For *PGE*, there is no increase in circuit depth,

and the ansatz remains constant regardless of the number of edges in the graph, only depending on the number of vertices. This implies that while the number of entanglement gates, remains fewer than the number of variables in the QUBO, the overall resource efficiency is maintained. The number of parameters, which corresponds directly to the number of pixels, represents the primary challenge for the classical optimizer due to its exponential relationship with the number of qubits. The consistency in circuit design across different graph connectivities suggests that *PGE* could benefit significantly from more intricate connections in the image-derived graph. Such enhancements could potentially improve the spatial information consideration for each pixel, enriching segmentation quality without adding computational overhead.

The methods *ABE* and *ACE* similarly display a significant reduction in quantum resource requirements for addressing NP-Hard segmentation problems, aligning with the conservation goals typical of near-term quantum technologies. These methods achieve scalability primarily through their linear increase in parameters with the number of layers, which enhances their applicability without exponential increases in resource demands. However, the number of circuit measurements scales exponentially with the number of qubits allowing us to measure the ancilla qubit state for all possible register basis states to obtain a complete binary vector solution. Experimentally, *ACE* has proven to achieve optimal solutions with increased layers and parameters, provided that a robust classical optimizer is used. This highlights the potential for optimizing the synergy between quantum circuit design and classical optimization techniques, advancing applications of quantum technology. Additionally, a deeper exploration of the optimization landscape could unveil methods allowing classical optimizers to find global optima more effectively.

In summary, the techniques covered here demonstrate the potential of new encoding schemes, allowing vital applications like image segmentation to benefit from emerging quantum technologies, even with the current limitations of hardware from the NISQ era. These developments highlight the crucial role that novel quantum computational techniques play in overcoming classical computational challenges and open up promising directions for future research into quantum-enhanced computer vision.

CODE AVAILABILITY

All code to generate the data, figures, analyses, as well as, additional technical details on the experiments are publicly available at https://github.com/supreethmv/NISQ-Seg.

REFERENCES

[1] M. Cerezo, A. Arrasmith, R. Babbush, S. C. Benjamin, S. Endo, K. Fujii, J. R. McClean, K. Mitarai, X. Yuan, L. Cincio, and P. J. Coles, "Variational quantum algorithms," *Nature Reviews Physics*, vol. 3, no. 9, pp. 625–644, Sep 2021. [Online]. Available: https://doi.org/10.1038/s42254-021-00348-9

[2] F. Glover, G. Kochenberger, and Y. Du, "Applications and computational advances for solving the qubo model," in *The Quadratic Unconstrained Binary Optimization Problem: Theory, Algorithms, and Applications*. Springer, 2022, pp. 39–56.

[3] E. Farhi, J. Goldstone, and S. Gutmann, "A quantum approximate optimization algorithm," 2014.

[4] M. J. Rančić, "Noisy intermediate-scale quantum computing algorithm for solving an n-vertex maxcut problem with $\log(n)$ qubits," *Phys. Rev. Res.*, vol. 5, p. L012021, Feb 2023. [Online]. Available: https://link.aps.org/doi/10.1103/PhysRevResearch.5.L012021

[5] B. Tan, M.-A. Lemonde, S. Thanasilp, J. Tangpanitanon, and D. G. Angelakis, "Qubit-efficient encoding schemes for binary optimisation problems," *Quantum*, vol. 5, p. 454, May 2021. [Online]. Available: https://doi.org/10.22331/q-2021-05-04-454

[6] S. M. Venkatesh, A. Macaluso, M. Nuske, M. Klusch, and A. Dengel, "Q-seg: Quantum annealing-based unsupervised image segmentation," 2023.

[7] O. Ronneberger, P.Fischer, and T. Brox, "U-net: Convolutional networks for biomedical image segmentation," in *Medical Image Computing and Computer-Assisted Intervention (MICCAI)*, ser. LNCS, vol. 9351. Springer, 2015, pp. 234–241, (available on arXiv:1505.04597 [cs.CV]). [Online]. Available: http://lmb.informatik.uni-freiburg.de/Publications/2015/RFB15a

[8] Y. Wang, J. Cheng, Y. Chen, S. Shao, L. Zhu, Z. Wu, T. Liu, and H. Zhu, "FVP: Fourier visual prompting for source-free unsupervised domain adaptation of medical image segmentation," *IEEE Transactions on Medical Imaging*, pp. 1–1, 2023. [Online]. Available: https://ieeexplore.ieee.org/document/10223270

[9] F. Yi and I. Moon, "Image segmentation: A survey of graph-cut methods," in *2012 international conference on systems and informatics (ICSAI2012)*. IEEE, 2012, pp. 1936–1941.

[10] H. Neven, G. Rose, and W. G. Macready, "Image recognition with an adiabatic quantum computer i. mapping to quadratic unconstrained binary optimization," *arXiv preprint arXiv:0804.4457*, 2008.

[11] H. Neven, V. S. Denchev, G. Rose, and W. G. Macready, "Training a binary classifier with the quantum adiabatic algorithm," *arXiv preprint arXiv:0811.0416*, 2008.

[12] H. Neven, V. S. Denchev, M. Drew-Brook, J. Zhang, W. G. Macready, and G. Rose, "Nips 2009 demonstration: Binary classification using hardware implementation of quantum annealing," *Quantum*, vol. 4, p. 1, 2009.

[13] E. Grant, M. Benedetti, S. Cao, A. Hallam, J. Lockhart, V. Stojevic, A. G. Green, and S. Severini, "Hierarchical quantum classifiers," *npj Quantum Information*, vol. 4, no. 1, p. 65, 2018.

[14] N. Jiang, Y. Dang, and J. Wang, "Quantum image matching," *Quantum Information Processing*, vol. 15, no. 9, pp. 3543–3572, Sep 2016. [Online]. Available: https://doi.org/10.1007/s11128-016-1364-2

[15] H. Bhatia, E. Tretschk, Z. Lähner, M. Seelbach Benkner, M. Möller, C. Theobalt, and V. Golyanik, "Ccuantumm: Cycle-consistent quantum-hybrid matching of multiple shapes," in *IEEE Conference on Computer Vision and Pattern Recognition (CVPR)*, 2023.

[16] Ç. Aytekin, S. Kiranyaz, and M. Gabbouj, "Quantum mechanics in computer vision: Automatic object extraction," in *2013 IEEE International Conference on Image Processing*. IEEE, 2013, pp. 2489–2493.

[17] S. Yuan, X. Mao, L. Chen, and Y. Xue, "Quantum digital image processing algorithms based on quantum measurement," *Optik*, vol. 124, no. 23, pp. 6386–6390, 2013.

[18] X. Fu, M. Ding, Y. Sun, and S. Chen, "A new quantum edge detection algorithm for medical images," in *MIPPR 2009: Medical Imaging, Parallel Processing of Images, and Optimization Techniques*, vol. 7497. SPIE, 2009, pp. 547–553.

[19] L. Tse, P. Mountney, P. Klein, and S. Severini, "Graph cut segmentation methods revisited with a quantum algorithm," *arXiv preprint arXiv:1812.03050*, 2018.

[20] T. Presles, C. Enderli, G. Burel, and E. H. Baghious, "Synthetic aperture radar image segmentation with quantum annealing," *IET Radar, Sonar & Navigation*, vol. n/a, no. n/a, p. 1–13, 2024. [Online]. Available: https://ietresearch.onlinelibrary.wiley.com/doi/abs/10.1049/rsn2.12523

[21] S. M. Venkatesh, A. Macaluso, and M. Klusch, "Gcs-q: Quantum graph coalition structure generation," in *Computational Science – ICCS 2023*, J. Mikyška, C. de Mulatier, M. Paszynski, V. V. Krzhizhanovskaya, J. J. Dongarra, and P. M. Sloot, Eds. Cham: Springer Nature Switzerland, 2023, pp. 138–152.

[22] A. Lucas, "Ising formulations of many np problems," *Frontiers in Physics*, vol. 2, p. 5, 2014, edited by Jacob Biamonte, ISI Foundation, Italy.

[23] F. Glover, G. Kochenberger, and Y. Du, "A tutorial on formulating and using qubo models," *arXiv preprint arXiv:1811.11538*, 2018.

[24] S. Gupta and V. Kekatos, "A quantum approach for stochastic constrained binary optimization," in *ICASSP 2023 - 2023 IEEE International Conference on Acoustics, Speech and Signal Processing (ICASSP)*, June 2023, pp. 1–5.

[25] S. M. Venkatesh, A. Macaluso, and M. Klusch, "Bilp-q: Quantum coalition structure generation," in *Proceedings of the 19th ACM International Conference on Computing Frontiers*, ser. CF '22. New York, NY, USA: Association for Computing Machinery, 2022, p. 189–192. [Online]. Available: https://doi.org/10.1145/3528416.3530235